Published in final edited form as:
Trends Neurosci. 2010 September ; 33(9): 415–423. doi:10.1016/j.tins.2010.06.004.

BK channel activation: structural and functional insights

Urvi S. Lee and **Jianmin Cui**
Department of Biomedical Engineering and Cardiac Bioelectricity and Arrhythmia Center, Washington University, St. Louis, MO 63130

Abstract

The voltage and Ca^{2+} activated K^+ (BK) channels are involved in the regulation of neurotransmitter release and neuronal excitability. Structurally, BK channels are homologous to voltage- and ligand-gated K^+ channels, having a voltage sensor and pore as the membrane-spanning domain and a cytosolic domain containing metal binding sites. Recently published electron cryomicroscopy (cryo-EM) and X-ray crystallographic structures of the BK channel provided the first look into the assembly of these domains, corroborating the close interactions among these domains during channel gating that have been suggested by functional studies. This review discusses these latest findings and an emerging new understanding about BK channel gating and implications for diseases such as epilepsy, in which mutations in BK channel genes have been associated.

BK channels

Large conductance Ca^{2+}-activated K^+ channels (BK channels, see also Box 1) have a large unitary conductance of ~100–300 pS and activate in response to membrane depolarization and binding of intracellular Ca^{2+} and Mg^{2+} [1–4]. The channel is formed by four pore-forming subunits that are encoded by a single *Slo1* gene [5–7]. BK channels achieve functional diversity primarily through alternative splicing of the *Slo1* mRNA and modulation by accessory β subunits [8–10]. There are four types of β subunits (β1-4); each type displays a distinct tissue-specific expression pattern and uniquely modifies gating properties of the channel [11–22]. β4 subunits are most exclusively expressed in the brain [12–15]. β2 and β3 subunits are also neuronally expressed, whereas the β1 subunit primarily distributes in smooth muscle cells [12–15].

Box 1

Nomenclature for BK channels. A variety of different names are used in discussions of BK channels

- Gene of the pore-forming subunit:
  - KCNMA1
  - Slo/Slo1
  - Slowpoke
- Protein of the pore-forming subunit:

Corresponding author: Cui, J. (jcui@biomed.wustl.edu).

- Slo1
- Alpha (α) subunit

- Functional channels (comprising four pore-forming subunits and auxiliary β subunits):
  - Large conductance Ca^{2+}-activated K^+ channels
  - Slo1 – only composed of the pore-forming subunit
  - Maxi-K
  - BK or BK_{Ca}
  - $K_{Ca}1.1$

In neurons such as those in hippocampus and cerebellum, the Slo1 subunit shows a specific distribution to the axons and presynaptic terminals [23–25], and BK channels are usually found in close proximity with voltage-gated Ca^{2+} channels [26–31]. During an action potential, membrane depolarization and Ca^{2+} entry through Ca^{2+} channels activate BK channels, which help to terminate the action potential, produce fast after-hyperpolarization and shut Ca^{2+} channels [11,32,33]. Through this negative feedback mechanism, BK channels regulate membrane excitability and intracellular Ca^{2+} signaling. Consequently, BK channels play an important role in controlling neurotransmitter release [34–38], fast after-hyperpolarization and are involved in spike frequency adaptation [39–42].

What are the structural domains of BK channels that are involved in sensing voltage, Ca^{2+} and Mg^{2+} ions? Furthermore, what are the mechanisms by which these domains open the channel gate to allow the influx of K^+ ions? These questions are key to understanding the physiological functions of BK channels. Recent functional studies, homology models, the electron cryomicroscopy (cryo-EM) and X-ray crystallographic structures of BK channels are enabling new insights into the biophysical underpinnings of BK channel gating. These latest findings will be discussed in this review, along with additional questions that emerge regarding the exact details of the structural domains that are important for BK channel gating as well as in neuronal physiology and pathophysiology.

Structural and functional domains of BK channels

The Slo1 subunit contains three main structural domains (Figure 1), with each domain serving a distinct function: the voltage sensing domain (VSD) senses membrane potential, the cytosolic domain senses Ca^{2+} ions, and the pore-gate domain (PGD) opens and closes to control K^+ permeation. The activation gate, which changes conformation during channel activation from restricting K^+ flux to permeating K^+ flux, resides in the PGD that may be located at either the cytosolic side of S6 [43] or the selectivity filter [43–46]. The VSD and PGD are collectively called the membrane-spanning domains and are formed by transmembrane segments S1-S4 and S5-S6, respectively [47], similar to voltage-gated K^+ channels. The S4 helix contains a series of positively charged residues and serves as the primary voltage sensor, which moves toward the extracellular side in response to membrane depolarization [5–7]. However, in BK channels only one of the charged residues (Arg213) has been shown to contribute to voltage sensing [48]. Also unique to BK channels is an additional S0 segment, which is required for β subunit modulation [17,49] and may function in modulating voltage sensitivity [50]. The cytosolic domain is comprised of two RCK (regulator of K^+ conductance) domains, RCK1 and RCK2 [51] (Figure 1). These domains contain two putative high affinity Ca^{2+} binding sites: one in the RCK1 domain at position Asp362/Asp367 (this numbering scheme is based on the mbr5 sequence of mouse α subunit) [52,53] and the other in a region termed the Ca^{2+} bowl

that contains a series of Asp residues [54,55], located in the RCK2 domain [51]. The Mg^{2+} binding site is at the interface between the VSD (Asp99 and Asn172) and cytosolic domain (Glu374 and Glu399) [52,53,56] (Figure 2B). In addition, other signaling molecules such as carbon monoxide [57] and heme [58–60] also modulate gating properties of the channel by interacting with residues in the cytosolic domain. While these studies have identified the sensors for voltage and metal ions, the results also show that these sensors and the activation gate are spatially separated. How the voltage and metal ion binding open the activation gate over this distance is not clear. In this article, we present results from recent studies that suggest the interactions between different structural domains are important for coupling the sensors to the activation gate.

Homology and structural models support interactions between the structural domains

Based on the homology of primary sequences and predicted secondary structures, structural models of BK channels have been constructed using the crystal structure of the mammalian $K_V1.2$ channel [61] as a template for the membrane-spanning domains, VSD and PGD [48, 56,62–65], and the structure of prokaryotic Ca^{2+}-gated K^+ channel, MthK, from *Methanobacterium thermoautotrophicum*, for the cytosolic domain [60,65–70]. Recently, the structure of the cytosolic domain of Slo1 has been solved and is used to construct the homology model of BK channels [51] (Figure 1C). The structure of the $K_V1.2$ channel revealed that S5 to S6 from four α subunits form a central pore with the VSDs positioned at four corners of the pore domain [61]. The VSD associates with the PGD via three major interactions (Figure 2A): (1) physical connection between the VSD and PGD through the S4-S5 linker [61,71,72] (2) interactions between the S4-S5 linker and the cytosolic side of S6 [71–75], and (3) interactions between S4 and S5 of a neighboring subunit [61,76,77]. All of these interactions may mediate the coupling between voltage sensor movements and the opening of the activation gate of K_V channels, and by analogy, BK channels [71–77]. In the MthK channel, each subunit contains two transmembrane segments that form the pore and eight identical cytosolic RCK domains that form the gating ring complex, where four of the eight RCK domains are tethered to the inner helices of the pore and the other four are independent and derived from an alternative initiation codon [66]. The RCK domain consists of alternating β strands and α helices, labeled as βA to αJ, which adopts a Rossmann-fold topology where the β sheets are sandwiched between the α helices. The N-terminal part of the eight RCK domains from βA to αF forms the core of the gating ring, while the C-terminal part froms αG to αJ form a C-terminal lobe [66,78]. Ca^{2+} binding to the gating ring induces an expansion of its diameter, which pulls the peptides tethered to the pore to open the channel [66,79]. A similar gating ring, formed by four pairs of RCK1 and RCK2 domains, exists in BK channels (Figure 1C) [51,78], where the RCK1 adopts a similar structure as the RCK domains in MthK and similar nomenclatures are used to describe the secondary structures, while the RCK2 structure is less conserved and the secondary structures are described by different nomenclatures [51].

Recently, a structure of the BK channel at 1.7–2.0 nm resolution was obtained using cryo-EM [80] (see also Ref. [81] for a recent review of the cryo-EM technique). The residues displayed on the extracellular face and the spatial dimension of the membrane-spanning region in the cyro-EM structure of the BK channel are similar to that of $K_V1.2$ [61,72] and a prokaryotic cyclic nucleotide-gated channel, MlotiK [82], congruent with the homology model of the VSD and PGD domains in BK channels [80]. Likewise, the MthK gating ring can be spatially overlapped with the BK channel structure, supporting the gating ring model of BK channels [80]. More recently, a crystal structure of the cytosolic domain of Slo1, including both RCK1 and RCK2, has been solved at 3.0 Å resolution [51]. In the same study, the tetrameric assembly of the gating ring of a homologous Na^+-sensitive Slo2 channel was also solved at 6 Å resolution

[51]. These structures indicate that the RCK1 and RCK2 domains from four Slo1 subunits indeed form a gating ring in BK channels similar to that of the MthK channel.

In addition, these structural results reveal important features that are unique to BK channels. First, compared to the $K_V1.2$ structure, the membrane-spanning domains of the cryo-EM BK structure contains an additional structural component, which is likely to account for the unique S0 segment in BK channels, as well as the N-terminus and S0-S1 linker that flank S0 [80]. The S0 segment is located at the periphery of the VSD, adjacent to the S2 domain, which is consistent with the results of previous studies using chemical cross-linking to detect the proximity of the S0 segment with other transmembrane segments [62,80]. At such a location, the S0 segment may not directly affect the interaction between S4 and the PGD within the membrane.

Second, the cytosolic domain of the BK channel is larger than that of MthK channels. Each RCK domain of the MthK channel contains 217 amino acids [66], while RCK 1 and RCK2 of the BK channel contain 266 and 376 amino acids, respectively [51]. Although RCK1 and RCK2 also adopt a Rossmann fold the gating ring in BK channels is larger than that in MthK along the central axis [51,80]. Similar to that in MthK, the gating ring in BK channels also contains an assembly interface and a flexible interface between RCK1 and RCK2, with the flexible interface formed by a helix-turn-helix from both RCK domains. However, the interface between the two RCK domains is more extensive in BK channels, indicating a highly specific and strong interaction between the two domains.

A third important feature that was revealed by the structural data is that the cytosolic domain is spatially close to the membrane-spanning domains. Overlapping the structures of $K_V1.2$ and the gating ring of MthK channels on the cryo-EM BK structure does not give rise to any gap between the two structures [80]. The crystal structure of the RCK1 domain can also fit well with the cytosolic face of the membrane-spanning domains [51]. This feature is consistent with previous functional studies [56,83] that suggest an intimate interaction between the VSD and cytosolic domain during BK channel gating.

The crystal structure of the Slo1 cytosolic domain reveals that the Ca^{2+} bowl is part of the RCK2 domain, and a strong electron density at the center of the Ca^{2+} bowl structure is consistent with a bound Ca^{2+} ion [51]. Unlike in the MthK channel where the Ca^{2+} binding sites are clustered at the flexible interface between adjacent RCK domains, the Ca^{2+} bowl is closer to the subunit-subunit interface known as the assembly interface in the gating ring complex. The crystal structure does not identify the second Ca^{2+} binding site in RCK1. Although Asp367 is clearly shown in the structure, no Ca^{2+} ion appears near the site albeit the structure was solved in 50 mM Ca^{2+}, a concentration that far exceeds the saturating concentration for this site as determined by functional studies (~100 μM) [52,84]. One possible reason for this result is that the membrane-spanning domains may influence the structure of this Ca^{2+} binding site in RCK1 so that the Ca^{2+} binding site cannot bind to Ca^{2+} in the crystal structure due to the lack of the interaction from the membrane-spanning domains. It was shown that mutations in the S0-S1 loop altered Ca^{2+} sensitivity of the channel [85], while in the cryo-EM BK channel structure the cytosolic S0-S1 loop is proposed to snugly fit in between the VSD and gating ring to fill the void between the core and C-terminal lobe (also known as the peripheral subdomain) of the gating ring [80]. In addition, the structure was solved in a solution with low pH (at pH 4.8), and the high concentration of protons may interfere with Ca^{2+} binding to the putative Asp367 site [86].

Evidence of interactions between structural domains

In the Slo1 subunit, the cytosolic domain is connected to S6 by a peptide linker of 17 amino acids, which is called the C-linker here. By altering the length of the C-linker by deleting amino

acids or inserting poly-AAG segments, it has been demonstrated that the activity of the BK channel is dependent on the C-linker length [87]. The channel is less active with increased Clinker length at the same voltage, both in the absence or presence of Ca^{2+} [87]. This data is consistent with a model that suggests that a tug of the S6 segment by the cytosolic domain, via the C-linker, opens the activation gate; a longer linker reduces the force and decreases the sensitivity to Ca^{2+} modulation [87]. This mechanism is similar to that observed in the MthK channel, where Ca^{2+} binding causes an expansion of the gating ring that pulls the linker connecting the gating ring to the inner helix of the pore to promote channel opening [66,79].

Besides interacting with the PGD, the cytosolic domain also intimately interacts with the VSD that mediates Mg^{2+}-dependent activation. The Mg^{2+} binding site is located at the interface between the VSD and cytosolic domain, formed by Asp99 in the S0-S1 loop, Asn172 in the cytosolic end of S2, and Glu374 and Glu399 in RCK1 (Figure 2B). In forming the Mg^{2+} binding site, two residues come from RCK1 of one Slo1 subunit and the other two residues come from the VSD of the neighboring subunit [56]. In order for these residues to coordinate the Mg^{2+} ion, the VSD and cytosolic domain from neighboring subunits must be in close proximity. To further demonstrate this, Asp99 in the VSD domain and Gln397 (which is close to Glu374 and Glu399) in the cytosolic domain were mutated to cysteine residues, where they spontaneously formed a disulfide bond [56]. This demonstrates that the proximate distance between these two residues is between 2.9 and 4.6 Å [56]. The bound Mg^{2+} ion activates the channel by interacting with the VSD via an electrostatic repulsion, with Arg213 located at the cytosolic end of S4 promoting channel opening [83]. Due to this interaction, it is more difficult for the gating charge to return to the resting state, resulting in a leftward shift of the Q (charge)-V (voltage) relationship [83]. This electrostatic repulsion of Arg213 by Mg^{2+} can be mimicked by a positive charge added to Gln397 via mutation or chemical modification [83]. A calculation based on this result indicates that the distance between Arg213 in the VSD domain and Gln397 in the cytosolic domain is at most 9.1Å [83]. These distances calculated from functional data need to be confirmed by high resolution structures that include both the membrane-spanning and cytosolic domains.

In BK channels, voltage sensor movements can be detected when the gate is either closed or open [88]. It has been shown that Mg^{2+} affects the movements of the voltage sensor more prominently when the channels are in the open state [83,89]. During a depolarizing voltage pulse, channel opening gradually increases until a steady state is reached; correspondingly, the off-gating currents, which measures the voltage sensor movement to the resting state, become smaller and decay at a slower rate [83]. This indicates that the electrostatic repulsion between the bound Mg^{2+} and the S4 segment becomes stronger as the channel opens. These results suggest that the opening of the activation gate in the PGD may alter the alignment between the VSD and cytosolic domain such that the bound Mg^{2+} ion is situated closer to the S4 segment. Thus, the activation gate may interact with the cytosolic domain, VSD, or both to cause such an alignment shift (Figure 2). Reciprocally, a shift in the alignment between the VSD and cytosolic domain should also affect the opening of the activation gate, although no evidence supporting this mechanism has been provided. Moreover, it is not clear if Mg^{2+} binding to the interface between the two domains facilitates such an alignment shift, which may contribute to Mg^{2+} dependent activation in addition to the electrostatic interactions between bound Mg^{2+} and the S4 segment.

The above evidence demonstrates that the cytosolic domain of BK channels interacts with the membrane-spanning domain not only by a tugging of the PGD via the C-linker but also by a nudging through side chain interactions at the VSD that are affected by the opening of the activation gate (Figure 2). In addition, a recent study suggested that although the four VSD in BK channels are separated at four corners along the rim of the PGD, the activation of these voltage sensors may be cooperative, and this cooperativity may arise from the interaction of

VSDs with the cytosolic domain [90]. Nevertheless, while these results fit well with the cryo-EM structure in which the cytosolic and membrane-spanning domains are located in close proximity, aqueous crevices exist where the domains may not directly interact. A central antechamber between the membrane-spanning and cytosolic domains has been shown to accommodate the N-terminus of the accessory β2 subunit, which blocks the pore and causes inactivation, and protects it from intracellular trypsin digestion [91,92]. This antechamber is spacious and large enough to accommodate the first 19 residues in the N-terminus of the β2 subunit since Arg19 was protected from trypsin digestion [91]. Therefore, the residues from the membrane-spanning and cytosolic domains, which line the wall of the antechamber, may not interact with each other. Interestingly, when the channel is in the closed state, the β2 N-terminal peptide binds to a site in the antechamber that differs from the site in the inactivated state, and fewer residues are accommodated in the antechamber [92]. These results suggest that the size of the antechamber may be altered during channel gating and some residues lining the walls may change distance and interactions during channel gating. However, the exact structures lining the inner face of the antechamber, how it extends in size, and whether its alteration during channel gating contributes energy to gating remain unclear.

Domain interactions in Ca^{2+} dependent activation

A prevalent model proposed for ion channel activation by intracellular ligands is that ligand binding alters the conformation of the cytosolic domain, which pulls to open the activation gate via a peptide linking the membrane-spanning domain to the cytosolic domain (a tugging model) [66,93–95]. On the other hand, in BK channels Mg^{2+} activates the channel by pushing the voltage sensor via an electrostatic interaction and involving the interaction among side chains in different structural domains (a nudging model). Since Ca^{2+} sensitivity of BK channels depends on the length of the C-linker [87], it has been suggested that Ca^{2+}activates the channel through a tugging model. However, recent results show that Ca^{2+} binding to the two different high affinity sites activates the channel with distinct properties, suggesting that the mechanisms underlying Ca^{2+} dependent activation via the two sites may be more complex.

The difference in Ca^{2+} binding sites was first noted in a study when the Ca^{2+} bowl was mutated, and it was found that the channel retained partial Ca^{2+} sensitivity and an intact sensitivity to Cd^{2+}. Based on these results, it was proposed that BK channels may contain a second Ca^{2+} binding site, which can also bind to Cd^{2+}, to activate the channel [54]. This proposal was verified later in a study to show that the putative second Ca^{2+} binding site in RCK1 (Asp362/Asp367, where Asp362 has a minor effect on Ca^{2+} sensitivity) is responsible for Cd^{2+} sensitivity of the channel [96]. More importantly, the affinity of Ca^{2+} for the two sites differs [52,84,97]. Estimated by measuring open probability of the channel in various intracellular Ca^{2+} concentrations ($[Ca^{2+}]_i$) and then fitting the data to the MWC allosteric model that was originally proposed by Monod, Wyman and Changeaux to describe the binding of oxygen to hemoglobin [98] and subsequently adopted to describe voltage and Ca^{2+} dependent activation of BK channels [99], the dissociation constant of Ca^{2+} at open (K_O) and closed (K_C) states are 5.6 μM and 26.8 μM for the site in RCK1, and 0.88 μM and 3.13 μM for the Ca^{2+} bowl [84]. In the MWC model, each Ca^{2+} ion binding to the channel favors the transition for channel opening by a factor $C = K_C/K_O$. Hence, Ca^{2+} binding to the site in RCK1 contributes more than binding to the Ca^{2+} bowl to activating the channel (C = 4.75 vs. 3.55) [52,84,100]. Corresponding to the difference in affinity, Ca^{2+} binding to the Ca^{2+} bowl and to the site in RCK1 is responsible for the increase of activation rate in 0–10 μM and 10–300 μM $[Ca^{2+}]_i$, respectively [96].

Besides these properties of the two Ca^{2+} binding sites, the mechanism of how these binding sites are coupled to the activation gate also differs. In a recent mutational scan, i.e. each residue is individually mutated, of the N-terminal region of the RCK1 domain from βA to αC (thus

called the AC region) mutations of ten residues are found to specifically alter the Ca^{2+} dependent activation originated from the site in RCK1 [100]. In the homology model of BK channels (e.g., Figure 1C), the AC region is located just beneath the membrane spanning domains like a pedestal; and it contains the putative Ca^{2+} binding site Asp362/Asp367 and the residues Glu374 and Glu399 that form the Mg^{2+} binding site with Asp99 and Asn372 in the membrane-spanning domain (Figure 2B). Interestingly, all ten residues, which alter Ca^{2+} sensitivity, are located at the surface of the AC region facing the membrane-spanning domains, which may interact with residues in the VSD and PGD to mediate the coupling between Ca^{2+} binding site in RCK1 and the activation gate [100]. An independent study showed that Ca^{2+} dependent activation originated from the binding site in RCK1, but not from the Ca^{2+} bowl, is affected by voltage, which also suggests that the AC region may interact with the VSD [84]. Taken together, these results suggest that a nudging model may be at least partially responsible for the activation of BK channels by Ca^{2+} binding to the site in RCK1 domain. Given the distinct locations of the two Ca^{2+} binding sites, where the Ca^{2+} bowl is located at the assembly interface between RCK1 and RCK2 and Asp367 is located close to the interface between RCK1 and the membrane-spanning domains [51], it is possible that the two binding sites may connect to the activation gate via different mechanisms.

BK channel dysfunction and neurological disorders

Achieving a better understanding of BK channel function is important not only for furthering our knowledge of the involvement of these channels in physiological processes, but also for pathophysiological conditions, as has been demonstrated by recent discoveries implicating these channels in neurological disorders. One such disorder is schizophrenia where BK channels are hypothesized to play a role in the etiology of the disease due to the effects of commonly used antipsychotic drugs on enhancing K^+ conductance [101]. Furthermore, this same study found that the mRNA expression levels of the BK channel were significantly lower in the prefrontal cortex of the schizophrenic group than in the control group [101]. Similarly, autism and mental retardation have been linked to haploinsufficiency of the *Slo1* gene and decreased BK channel expression [102].

Two mutations in BK channel genes have been associated with epilepsy. One mutation has been identified on the accessory β3 subunit, which results in an early truncation of the protein and has been significantly correlated in patients with idiopathic generalized epilepsy [103]. The other mutation is located on the *Slo1* gene, and was identified through genetic screening of a family with generalized epilepsy and paroxysmal dyskinesia [104]. The biophysical properties of this Slo1 mutation indicates enhanced sensitivity to Ca^{2+} and an increased average time that the channel remains open [104–107]. This increased Ca^{2+} sensitivity is dependent on the specific type of β subunit associating with the BK channel [106,107]. In association with the β3 subunit, the mutation does not alter the Ca^{2+}-dependent properties of the channel, but with the β4 subunit the mutation increases the Ca^{2+} sensitivity [105–107]. This is significant considering the relatively high abundance of the β4 subunit compared to the weak distribution of the β3 subunit in the brain [12,13,15,106,107]. It has been proposed that a gain of BK channel function may result in increases in the firing frequency due to rapid repolarization of APs, which allows a quick recovery of Na^+ channels from inactivation, thereby facilitating the firing of subsequent APs [104]. Supporting this hypothesis, mice null for the β4 subunit showed enhanced Ca^{2+} sensitivity of BK channels, resulting in temporal lobe epilepsy, which was likely due to a shortened duration and increased frequency of APs [108]. An interesting relevance to the mechanisms of BK channel activation as discussed above, the Slo1 mutation associated with epilepsy only alters Ca^{2+} dependent activation originated from the Ca^{2+} binding site in RCK1, but not from the Ca^{2+} bowl, by altering the coupling mechanism between Ca^{2+} binding and gate opening [100]. Since Ca^{2+} dependent activation originated from the Ca^{2+} binding site in RCK1 is enhanced by membrane depolarization, at the peak of an action

potential the binding of Ca^{2+} to the site in RCK1 contributes much more than binding to the Ca^{2+} bowl to activating the channel [84,109].

Although these associations between specific mutations in BK channel subunits and various neurological disorders have been demonstrated by numerous studies, it is also important to point out certain caveats with these studies, such as genetic linkage between BK channels and different diseases do not necessary show causation as these studies were performed based on correlation between changes in the protein/genetic marker and overall phenotype. Furthermore, studies performed using a mouse model also can fail to indicate what may happen in higher-order species, and this is especially true for BK channels, where certain β subunits are only primate specific [110].

Conclusion

Since the initial discovery of BK channels three decades ago (see [65]) recent advancements have led to the identification of the residues and functional units responsible for ligand and voltage sensing of BK channels and the development of an allosteric gating model to explain the channel's functional properties [111]. However, we are just beginning to understand the complex molecular interactions that couple the voltage and ligand sensors to the spatially distant activation gate. The recently published cryo-EM and X-ray crystallographic structures of the BK channel have provided the first look into the assembly of the quaternary structure of this massive channel protein. The structure corroborates the close interactions among the PGD, VSD and cytosolic domain that have been suggested by previous functional studies. These recent results indicate that the interactions among the structural domains of the BK channel are critical in coupling voltage sensor and metal ion binding sites to the activation gate. Deciphering the exact details of the molecular mechanisms underlying the gating of BK channels will be beneficial for achieving a better understanding of not only the general principles for ion channel gating but also the pathophysiological conditions where mutations in BK channels have been implicated.

Box 2

Organization in the potassium channel family. Potassium channels are categorized according to the number of transmembrane (TM) segments in the pore-forming α subunit

- 6 TM channels include a single pore and a voltage-sensing domain
  - Voltage-gated K^+ channels (K_V1.x-12.x)

    e.g. Shaker-related (K_V1.x-K_V4.x)
  - BK channels are a special member of this subfamily
- 4 TM channels include two pores
  - Leak channels (K_{2P}1.x-7.x, K_{2P}9.x-13.x, K_{2P}15.x-18.x)
- 2 TM channels include a single pore
  - Inwardly rectifying K^+ channels (K_{ir}1.x-7.x)
  - The MthK channel belongs to this family.

Acknowledgments

We thank Dr. Huanghe Yang for help in creating figures and Di Wu, Junqiu Yang and Mark Zaydman for their insightful comments. We thank Dr. Roderick MacKinnon for providing coordinates for the BK channel gating ring structure in Figure 1C. This work was supported by National Institutes of Health grants R01-HL70393 and R01-NS060706 to J.C. J.C. is an Associate Professor of Biomedical Engineering on the Spencer T. Olin Endowment.

References

1. Marty A. Ca-dependent K channels with large unitary conductance in chromaffin cell membranes. Nature 1981;291:497–500. [PubMed: 6262657]
2. Latorre R, Miller C. Conduction and selectivity in potassium channels. J Membr Biol 1983;71:11–30. [PubMed: 6300405]
3. Latorre R, et al. Varieties of calcium-activated potassium channels. Annu Rev Physiol 1989;51:385–399. [PubMed: 2653189]
4. Golowasch J, et al. Allosteric effects of Mg^{2+} on the gating of Ca^{2+}-activated K^{+} channels from mammalian skeletal muscle. J Exp Biol 1986;124:5–13. [PubMed: 2428908]
5. Adelman JP, et al. Calcium-activated potassium channels expressed from cloned complementary DNAs. Neuron 1992;9:209–216. [PubMed: 1497890]
6. Atkinson NS, et al. A component of calcium-activated potassium channels encoded by the Drosophila slo locus. Science 1991;253:551–555. [PubMed: 1857984]
7. Butler A, et al. mSlo, a complex mouse gene encoding “maxi” calcium-activated potassium channels. Science 1993;261:221–224. [PubMed: 7687074]
8. Navaratnam DS, et al. Differential distribution of Ca2+-activated K+ channel splice variants among hair cells along the tonotopic axis of the chick cochlea. Neuron 1997;19:1077–1085. [PubMed: 9390520]
9. Rosenblatt KP, et al. Distribution of Ca2+-activated K+ channel isoforms along the tonotopic gradient of the chicken’s cochlea. Neuron 1997;19:1061–1075. [PubMed: 9390519]
10. Tseng-Crank J, et al. Cloning, expression, and distribution of functionally distinct Ca(2+)-activated K+ channel isoforms from human brain. Neuron 1994;13:1315–1330. [PubMed: 7993625]
11. Orio P, et al. New disguises for an old channel: MaxiK channel beta-subunits. News Physiol Sci 2002;17:156–161. [PubMed: 12136044]
12. Behrens R, et al. hKCNMB3 and hKCNMB4, cloning and characterization of two members of the large-conductance calcium-activated potassium channel beta subunit family. FEBS Lett 2000;474:99–106. [PubMed: 10828459]
13. Brenner R, et al. Cloning and functional characterization of novel large conductance calcium-activated potassium channel beta subunits, hKCNMB3 and hKCNMB4. J Biol Chem 2000;275:6453–6461. [PubMed: 10692449]
14. Tseng-Crank J, et al. Cloning, expression, and distribution of a Ca(2+)-activated K+ channel beta-subunit from human brain. Proc Natl Acad Sci U S A 1996;93:9200–9205. [PubMed: 8799178]
15. Uebele VN, et al. Cloning and functional expression of two families of beta-subunits of the large conductance calcium-activated K+ channel. J Biol Chem 2000;275:23211–23218. [PubMed: 10766764]
16. Meera P, et al. A calcium switch for the functional coupling between alpha (hslo) and beta subunits (KV, Ca beta) of maxi K channels. FEBS Lett 1996;382:84–88. [PubMed: 8612769]
17. Wallner M, et al. Determinant for beta-subunit regulation in high-conductance voltage-activated and Ca(2+)-sensitive K+ channels: an additional transmembrane region at the N terminus. Proc Natl Acad Sci U S A 1996;93:14922–14927. [PubMed: 8962157]
18. Ding JP, et al. Inactivating BK channels in rat chromaffin cells may arise from heteromultimeric assembly of distinct inactivation-competent and noninactivating subunits. Biophys J 1998;74:268–289. [PubMed: 9449328]
19. Lingle CJ, et al. Inactivation of BK channels mediated by the NH(2) terminus of the beta3b auxiliary subunit involves a two-step mechanism: possible separation of binding and blockade. J Gen Physiol 2001;117:583–606. [PubMed: 11382808]

20. Solaro CR, et al. Inactivating and noninactivating Ca^{2+}- and voltage-dependent K^{+} current in rat adrenal chromaffin cells. J Neurosci 1995;15:6110–6123. [PubMed: 7545225]
21. Wang B, Brenner R. An S6 mutation in BK channels reveals beta1 subunit effects on intrinsic and voltage-dependent gating. J Gen Physiol 2006;128:731–744. [PubMed: 17130522]
22. Wang B, et al. Mechanism of beta4 subunit modulation of BK channels. J Gen Physiol 2006;127:449–465. [PubMed: 16567466]
23. Misonou H, et al. Immunolocalization of the Ca2+-activated K+ channel Slo1 in axons and nerve terminals of mammalian brain and cultured neurons. J Comp Neurol 2006;496:289–302. [PubMed: 16566008]
24. Knaus HG, et al. Distribution of high-conductance Ca(2+)-activated K+ channels in rat brain: targeting to axons and nerve terminals. J Neurosci 1996;16:955–963. [PubMed: 8558264]
25. Sausbier U, et al. Ca2+-activated K+ channels of the BK-type in the mouse brain. Histochem Cell Biol 2006;125:725–741. [PubMed: 16362320]
26. Grunnet M, Kaufmann WA. Coassembly of big conductance Ca2+-activated K+ channels and L-type voltage-gated Ca2+ channels in rat brain. J Biol Chem 2004;279:36445–36453. [PubMed: 15210719]
27. Berkefeld H, et al. BKCa-Cav channel complexes mediate rapid and localized Ca2+-activated K+ signaling. Science 2006;314:615–620. [PubMed: 17068255]
28. Fakler B, Adelman JP. Control of K(Ca) channels by calcium nano/microdomains. Neuron 2008;59:873–881. [PubMed: 18817728]
29. Wisgirda ME, Dryer SE. Functional dependence of Ca(2+)-activated K+ current on L- and N-type Ca2+ channels: differences between chicken sympathetic and parasympathetic neurons suggest different regulatory mechanisms. Proc Natl Acad Sci U S A 1994;91:2858–2862. [PubMed: 8146200]
30. Gola M, Crest M. Colocalization of active KCa channels and Ca2+ channels within Ca2+ domains in helix neurons. Neuron 1993;10:689–699. [PubMed: 8386529]
31. Marrion NV, Tavalin SJ. Selective activation of Ca2+-activated K+ channels by co-localized Ca2+ channels in hippocampal neurons. Nature 1998;395:900–905. [PubMed: 9804423]
32. Lancaster B, Nicoll RA. Properties of two calcium-activated hyperpolarizations in rat hippocampal neurones. J Physiol (Lond) 1987;389:187–203. [PubMed: 2445972]
33. Storm JF. Action potential repolarization and a fast after-hyperpolarization in rat hippocampal pyramidal cells. J Physiol 1987;385:733–759. [PubMed: 2443676]
34. Wang ZW. Regulation of synaptic transmission by presynaptic CaMKII and BK channels. Mol Neurobiol 2008;38:153–166. [PubMed: 18759010]
35. Salkoff L, et al. High-conductance potassium channels of the SLO family. Nat Rev Neurosci 2006;7:921–931. [PubMed: 17115074]
36. Raffaelli G, et al. BK potassium channels control transmitter release at CA3-CA3 synapses in the rat hippocampus. J Physiol 2004;557:147–157. [PubMed: 15034127]
37. Hu H, et al. Presynaptic Ca^{2+}-activated K^{+} channels in glutamatergic hippocampal terminals and their role in spike repolarization and regulation of transmitter release. J Neurosci 2001;21:9585–9597. [PubMed: 11739569]
38. Robitaille R, Charlton MP. Presynaptic calcium signals and transmitter release are modulated by calcium-activated potassium channels. J Neurosci 1992;12:297–305. [PubMed: 1370323]
39. Gu N, et al. BK potassium channels facilitate high-frequency firing and cause early spike frequency adaptation in rat CA1 hippocampal pyramidal cells. J Physiol (Lond) 2007;580:859–882. [PubMed: 17303637]
40. Greffrath W, et al. Contribution of Ca2+-activated K+ channels to hyperpolarizing after-potentials and discharge pattern in rat supraoptic neurones. J Neuroendocrinol 2004;16:577–588. [PubMed: 15214861]
41. Faber ES, Sah P. Calcium-activated potassium channels: multiple contributions to neuronal function. Neuroscientist 2003;9:181–194. [PubMed: 15065814]
42. Shao LR, et al. The role of BK-type Ca2+-dependent K+ channels in spike broadening during repetitive firing in rat hippocampal pyramidal cells. J Physiol 1999;521(Pt 1):135–146. [PubMed: 10562340]

43. Yellen G. The voltage-gated potassium channels and their relatives. Nature 2002;419:35–42. [PubMed: 12214225]
44. Wilkens CM, Aldrich RW. State-independent block of BK channels by an intracellular quaternary ammonium. J Gen Physiol 2006;128:347–364. [PubMed: 16940557]
45. Piskorowski RA, Aldrich RW. Relationship between pore occupancy and gating in BK potassium channels. J Gen Physiol 2006;127:557–576. [PubMed: 16636204]
46. Flynn GE, Zagotta WN. Conformational changes in S6 coupled to the opening of cyclic nucleotide-gated channels. Neuron 2001;30:689–698. [PubMed: 11430803]
47. Meera P, et al. Large conductance voltage- and calcium-dependent K+ channel, a distinct member of voltage-dependent ion channels with seven N-terminal transmembrane segments (S0-S6), an extracellular N terminus, and an intracellular (S9-S10) C terminus. Proc Natl Acad Sci U S A 1997;94:14066–14071. [PubMed: 9391153]
48. Ma Z, et al. Role of charged residues in the S1-S4 voltage sensor of BK channels. J Gen Physiol 2006;127:309–328. [PubMed: 16505150]
49. Morrow JP, et al. Defining the BK channel domains required for beta1-subunit modulation. Proc Natl Acad Sci U S A 2006;103:5096–5101. [PubMed: 16549765]
50. Koval OM, et al. A role for the S0 transmembrane segment in voltage-dependent gating of BK channels. J Gen Physiol 2007;129:209–220. [PubMed: 17296928]
51. Yuan P, et al. Structure of the Human BK Channel Ca2+-Activation Apparatus at 3.0 A Resolution. Science. 2010
52. Xia XM, et al. Multiple regulatory sites in large-conductance calcium-activated potassium channels. Nature 2002;418:880–884. [PubMed: 12192411]
53. Shi J, et al. Mechanism of magnesium activation of calcium-activated potassium channels. Nature 2002;418:876–880. [PubMed: 12192410]
54. Schreiber M, Salkoff L. A novel calcium-sensing domain in the BK channel. Biophys J 1997;73:1355–1363. [PubMed: 9284303]
55. Moczydlowski EG. BK channel news: full coverage on the calcium bowl. J Gen Physiol 2004;123:471–473. [PubMed: 15111642]
56. Yang H, et al. Activation of Slo1 BK channels by Mg2+ coordinated between the voltage sensor and RCK1 domains. Nat Struct Mol Biol 2008;15:1152–1159. [PubMed: 18931675]
57. Hou S, et al. The RCK1 high-affinity Ca^{2+} sensor confers carbon monoxide sensitivity to Slo1 BK channels. Proc Natl Acad Sci U S A 2008;105:4039–4043. [PubMed: 18316727]
58. Horrigan FT, et al. Heme Regulates Allosteric Activation of the Slo1 BK Channel. J Gen Physiol 2005;126:7–21. [PubMed: 15955873]
59. Lu R, et al. MaxiK channel partners: physiological impact. J Physiol (Lond) 2006;570:65–72. [PubMed: 16239267]
60. Tang XD, et al. Haem can bind to and inhibit mammalian calcium-dependent Slo1 BK channels. Nature 2003;425:531–535. [PubMed: 14523450]
61. Long SB, et al. Crystal structure of a mammalian voltage-dependent Shaker family K+ channel. Science 2005;309:897–903. [PubMed: 16002581]
62. Liu G, et al. Position and role of the BK channel alpha subunit S0 helix inferred from disulfide crosslinking. J Gen Physiol 2008;131:537–548. [PubMed: 18474637]
63. Liu G, et al. Locations of the beta1 transmembrane helices in the BK potassium channel. Proc Natl Acad Sci U S A 2008;105:10727–10732. [PubMed: 18669652]
64. Wu RS, et al. Location of the beta 4 transmembrane helices in the BK potassium channel. J Neurosci 2009;29:8321–8328. [PubMed: 19571123]
65. Cui J, et al. Molecular mechanisms of BK channel activation. Cell Mol Life Sci 2009;66:852–875. [PubMed: 19099186]
66. Jiang Y, et al. Crystal structure and mechanism of a calcium-gated potassium channel. Nature 2002;417:515–522. [PubMed: 12037559]
67. Latorre R, Brauchi S. Large conductance Ca^{2+}-activated K^{+} (BK) channel: activation by Ca^{2+} and voltage. Biol Res 2006;39:385–401. [PubMed: 17106573]

68. Kim HJ, et al. Modulation of the conductance-voltage relationship of the BK Ca channel by mutations at the putative flexible interface between two RCK domains. Biophys J 2008;94:446–456. [PubMed: 17890381]
69. Kim HJ, et al. Hydrophobic interface between two regulators of K+ conductance domains critical for calcium-dependent activation of large conductance Ca2+-activated K+ channels. J Biol Chem 2006;281:38573–38581. [PubMed: 17040919]
70. Yusifov T, et al. The RCK2 domain of the human BKCa channel is a calcium sensor. Proc Natl Acad Sci U S A 2008;105:376–381. [PubMed: 18162557]
71. Lu Z, et al. Ion conduction pore is conserved among potassium channels. Nature 2001;413:809–813. [PubMed: 11677598]
72. Long SB, et al. Voltage sensor of Kv1.2: structural basis of electromechanical coupling. Science 2005;309:903–908. [PubMed: 16002579]
73. Tristani-Firouzi M, et al. Interactions between S4-S5 linker and S6 transmembrane domain modulate gating of HERG K+ channels. J Biol Chem 2002;277:18994–19000. [PubMed: 11864984]
74. Lu Z, et al. Coupling between voltage sensors and activation gate in voltage-gated K+ channels. J Gen Physiol 2002;120:663–676. [PubMed: 12407078]
75. Lee SY, et al. Two separate interfaces between the voltage sensor and pore are required for the function of voltage-dependent K(+) channels. PLoS Biol 2009;7:e47. [PubMed: 19260762]
76. Soler-Llavina GJ, et al. Functional interactions at the interface between voltage-sensing and pore domains in the Shaker K(v) channel. Neuron 2006;52:623–634. [PubMed: 17114047]
77. Ledwell JL, Aldrich RW. Mutations in the S4 region isolate the final voltage-dependent cooperative step in potassium channel activation. J Gen Physiol 1999;113:389–414. [PubMed: 10051516]
78. Jiang Y, et al. Structure of the RCK domain from the E. coli K+ channel and demonstration of its presence in the human BK channel. Neuron 2001;29:593–601. [PubMed: 11301020]
79. Ye S, et al. Crystal structures of a ligand-free MthK gating ring: insights into the ligand gating mechanism of K^+ channels. Cell 2006;126:1161–1173. [PubMed: 16990139]
80. Wang L, Sigworth FJ. Structure of the BK potassium channel in a lipid membrane from electron cryomicroscopy. Nature 2009;461:292–295. [PubMed: 19718020]
81. Frank J. Single-particle reconstruction of biological macromolecules in electron microscopy--30 years. Q Rev Biophys 2009;42:139–158. [PubMed: 20025794]
82. Clayton GM, et al. Structure of the transmembrane regions of a bacterial cyclic nucleotide-regulated channel. Proc Natl Acad Sci U S A 2008;105:1511–1515. [PubMed: 18216238]
83. Yang H, et al. Mg2+ mediates interaction between the voltage sensor and cytosolic domain to activate BK channels. Proc Natl Acad Sci U S A 2007;104:18270–18275. [PubMed: 17984060]
84. Sweet TB, Cox DH. Measurements of the BKCa channel's high-affinity Ca2+ binding constants: effects of membrane voltage. J Gen Physiol 2008;132:491–505. [PubMed: 18955592]
85. Braun AP, Sy L. Contribution of potential EF hand motifs to the calcium-dependent gating of a mouse brain large conductance, calcium-sensitive K(+) channel. J Physiol 2001;533:681–695. [PubMed: 11410626]
86. Hou S, et al. Reciprocal regulation of the Ca^{2+} and H^+ sensitivity in the SLO1 BK channel conferred by the RCK1 domain. Nat Struct Mol Biol 2008;15:403–410. [PubMed: 18345016]
87. Niu X, et al. Linker-gating ring complex as passive spring and Ca(2+)-dependent machine for a voltage- and Ca(2+)-activated potassium channel. Neuron 2004;42:745–756. [PubMed: 15182715]
88. Horrigan FT, Aldrich RW. Allosteric voltage gating of potassium channels II. Mslo channel gating charge movement in the absence of Ca(2+). J Gen Physiol 1999;114:305–336. [PubMed: 10436004]
89. Horrigan FT, Ma Z. Mg2+ enhances voltage sensor/gate coupling in BK channels. J Gen Physiol 2008;131:13–32. [PubMed: 18166624]
90. Shelley C, et al. Coupling and cooperativity in voltage activation of a limited-state BK channel gating in saturating Ca2+ J Gen Physiol 2010;135:461–480. [PubMed: 20421372]
91. Zhang Z, et al. A limited access compartment between the pore domain and cytosolic domain of the BK channel. J Neurosci 2006;26:11833–11843. [PubMed: 17108156]

92. Zhang Z, et al. N-terminal inactivation domains of beta subunits are protected from trypsin digestion by binding within the antechamber of BK channels. J Gen Physiol 2009;133:263–282. [PubMed: 19237592]

93. Schumacher MA, et al. Structure of the gating domain of a Ca2+-activated K+ channel complexed with Ca2+/calmodulin. Nature 2001;410:1120–1124. [PubMed: 11323678]

94. Nishida M, et al. Crystal structure of a Kir3.1-prokaryotic Kir channel chimera. EMBO J 2007;26:4005–4015. [PubMed: 17703190]

95. Zagotta WN, Siegelbaum SA. Structure and function of cyclic nucleotide-gated channels. Annu Rev Neurosci 1996;19:235–263. [PubMed: 8833443]

96. Zeng XH, et al. Divalent cation sensitivity of BK channel activation supports the existence of three distinct binding sites. J Gen Physiol 2005;125:273–286. [PubMed: 15738049]

97. Bao L, et al. Elimination of the BK(Ca) channel's high-affinity Ca(2+) sensitivity. J Gen Physiol 2002;120:173–189. [PubMed: 12149279]

98. Monod J, et al. On the Nature of Allosteric Transitions: A Plausible Model. J Mol Biol 1965;12:88–118. [PubMed: 14343300]

99. Cox DH, et al. Allosteric gating of a large conductance Ca-activated K+ channel. J Gen Physiol 1997;110:257–281. [PubMed: 9276753]

100. Yang J, et al. An epilepsy/dyskinesia-associated mutation enhances BK channel activation by potentiating Ca2+ sensing. Neuron. 2010 (in press).

101. Zhang L, et al. Possible role of potassium channel, big K in etiology of schizophrenia. Med Hypotheses 2006;67:41–43. [PubMed: 16446048]

102. Laumonnier F, et al. Association of a functional deficit of the BKCa channel, a synaptic regulator of neuronal excitability, with autism and mental retardation. Am J Psychiatry 2006;163:1622–1629. [PubMed: 16946189]

103. Lorenz S, et al. Allelic association of a truncation mutation of the KCNMB3 gene with idiopathic generalized epilepsy. Am J Med Genet B Neuropsychiatr Genet 2007;144B:10–13. [PubMed: 16958040]

104. Du W, et al. Calcium-sensitive potassium channelopathy in human epilepsy and paroxysmal movement disorder. Nat Genet 2005;37:733–738. [PubMed: 15937479]

105. Diez-Sampedro A, et al. Mechanism of increased open probability by a mutation of the BK channel. J Neurophysiol 2006;96:1507–1516. [PubMed: 16738211]

106. Lee US, Cui J. {beta} subunit-specific modulations of BK channel function by a mutation associated with epilepsy and dyskinesia. J Physiol 2009;587:1481–1498. [PubMed: 19204046]

107. Wang B, et al. Mechanism of increased BK channel activation from a channel mutation that causes epilepsy. J Gen Physiol 2009;133:283–294. [PubMed: 19204188]

108. Brenner R, et al. BK channel beta4 subunit reduces dentate gyrus excitability and protects against temporal lobe seizures. Nat Neurosci 2005;8:1752–1759. [PubMed: 16261134]

109. Rothberg BS. Return of the electric binding site. J Gen Physiol 2008;132:487–489. [PubMed: 18955591]

110. Zeng X, et al. Species-specific Differences among KCNMB3 BK beta3 auxiliary subunits: some beta3 N-terminal variants may be primate-specific subunits. J Gen Physiol 2008;132:115–129. [PubMed: 18591419]

111. Horrigan FT, Aldrich RW. Coupling between voltage sensor activation, Ca2+ binding and channel opening in large conductance (BK) potassium channels. J Gen Physiol 2002;120:267–305. [PubMed: 12198087]

112. Long SB, et al. Atomic structure of a voltage-dependent K+ channel in a lipid membrane-like environment. Nature 2007;450:376–382. [PubMed: 18004376]

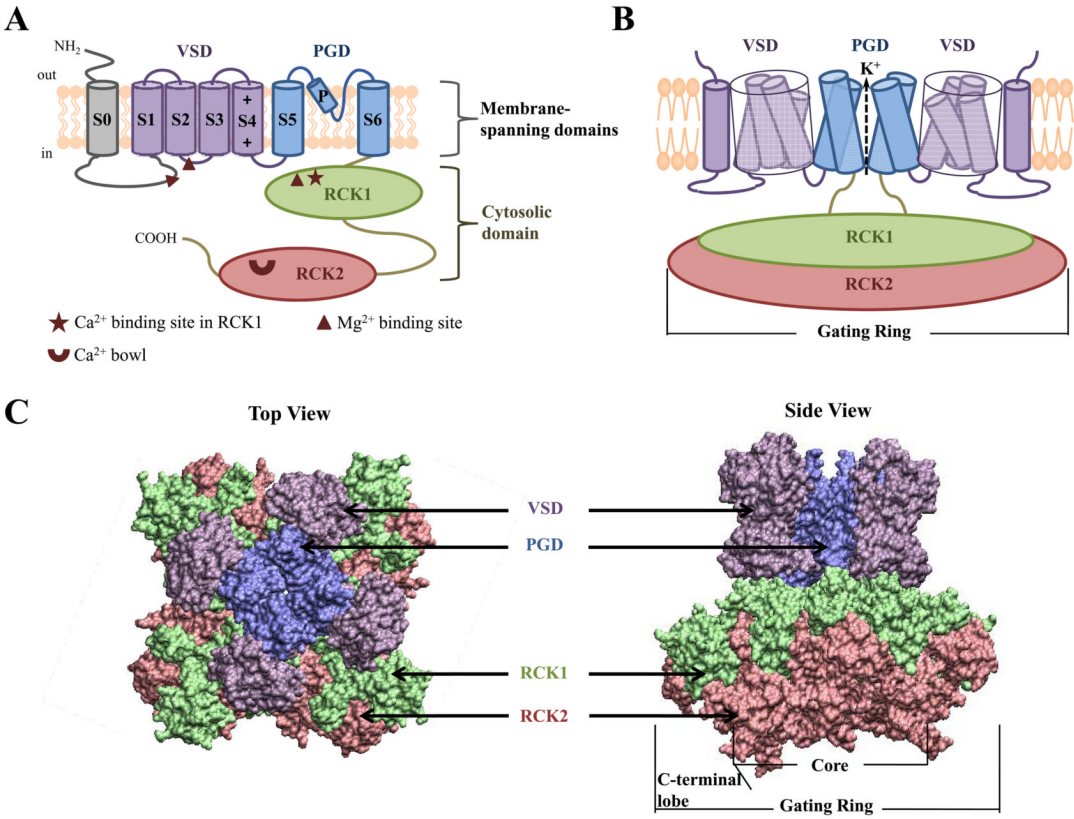

Figure 1.

BK channel structure. A) Membrane topology of the Slo1 subunit of BK channels, which highlights the S0 segment, voltage sensing domain (VSD; S1-S4 segments), pore-gate domain (PGD; S5, P and S6 segments) and cytosolic domain (RCK1 and RCK2). The positively charged residues in S4, and the Ca^{2+} and Mg^{2+} binding sites are indicated. B) Cartoon of a functional BK channel where two opposing subunits are shown for clarity. Similar color scheme as in (A) is used to identify different structural domains except for S0, which now has same color as the VSD. C) A homology model of the BK channel. The model was constructed by superimposing the crystal structures of the $K_V1.2$-$K_V2.1$ chimera in which the voltage-sensor paddle has been transferred from $K_V2.1$ to $K_V1.2$ (PDB ID: 2R9R) [112] and the MthK channel (PDB ID: 1LNQ) from *Methanobacterium thermoautotrophicum* [66] at the selectivity filter, and then superimposing the BK channel gating ring (PDB ID: 3MT5) [51] onto that of the MthK channel. Different structural domains of BK channels are depicted in surface representation, with the same color scheme as in (A) and (B). Left: top view as seen from the extracellular side. Right: side view. The model was constructed using UCSF Chimera v1.4.1 to superimpose the structures and VMD v1.8.7 to show them in surface representation.

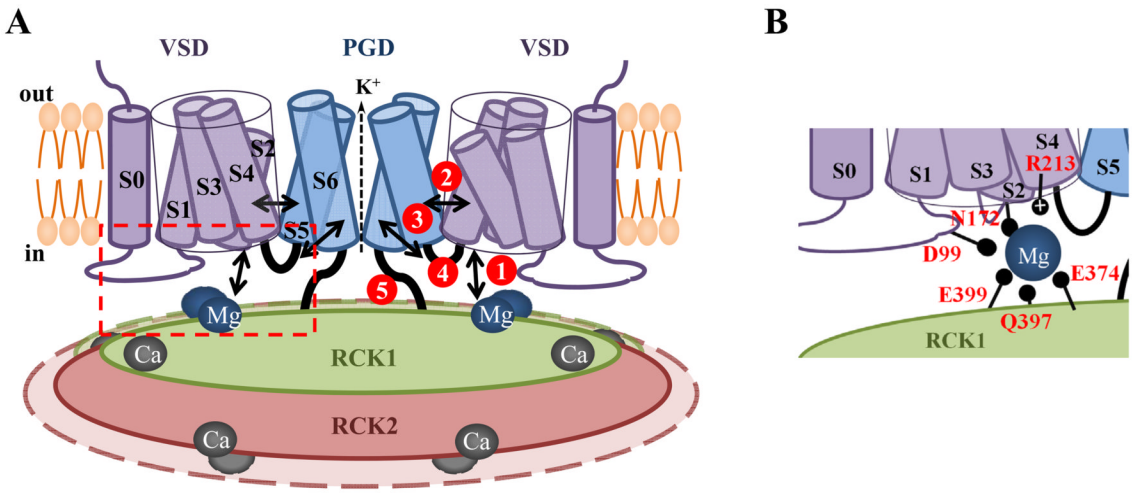

Figure 2.

Interactions between structural domains in BK channels. A) Cartoon of the BK channel. Mg^{2+} and Ca^{2+} show metal binding sites. Black arrows and heavy set lines are used to indicate the following interactions: 1) between VSD and RCK1 in Mg^{2+} dependent activation; 2) between VSD and PGD through S4 and S5; 3) between S4-S5 linker and S6; 4) the tug of the S4-S5 linker and 5) between PGD and cytosolic domain through the peptide C-linker. The gating ring formed by RCK1 and RCK2 is shown to undergo expansion during channel gating similar to the MthK channel from *Methanobacterium thermoautotrophicum*. The structure in dashed box is shown in more details in B. B) Cartoon showing residues involved in Mg^{2+} dependent activation.